Design of Power Converter Devices embedded in a Hybrid Emergency Network for More Electrical Aircraft

Rémy Rigo Mariani, Fabien Lacressonnière, Guillaume Fontes, Xavier Roboam

Design of Power Converter Devices embedded in a Hybrid Emergency Network for More Electrical Aircraft

R. Rigo Mariani, F. Lacressonniere, G. Fontes, X. Roboam

Université de Toulouse; LAPLACE (Laboratoire Plasma et Conversion d'Energie) UMR CNRS-INPT-UPS; ENSEEIHT, 2 rue Charles Camichel, BP 7122, F-31071 Toulouse cedex 7, France.

remy.rigo-mariani@laplace.univ-tlse.fr

Abstract - This paper deals with an emergency electrical network hybridized by electrochemical accumulators. Depending on the voltage of that storage device, different network topologies with different power converter structures and sizing have to be considered. This study mainly focuses on the design of DC-DC power converters trying to be as exhaustive as possible in view of determining the best voltage connection in terms of mass and efficiency.

Keywords – Power Converter Design, Sizing, efficiency, mass, Hybridization, emergency, electrical network, Aerospace

1. INTRODUCTİON

Judging from the changes that occurred in many subsystems with the concept of "More Electrical Aircraft" it becomes necessary to deeply refund electrical embedded networks [1]. This paper especially focuses on the emergency sub-network in which energy generation is classically ensured by a high speed turbine (Ram Air Turbine – RAT) that unfolds in case of electric generation or engine failure. A recent study demonstrated that a significant reduction could be expected in terms of weight and volume of that emergency subsystem (around 30%) by hybridizing the RAT with a storage device [2]. Hybridization is based on the principle of power sharing where the average power is supplied by the main power source (i.e the RAT) while transient load is fed by the storage device. Thus several solutions such as supercapacitors [3], or batteries are considered as storage device which has to be connected to the electrical network. That connection is directly linked to the whole architecture of the considered network. In this paper we face to a structure with two insulated DC buses:

- A 540V HVDC (High Voltage Direct Current) bus that feds the heavy loads such as flight controls surfaces (FC), de-ice or emergency braking for a maximum consumption estimated to 27kW. These essential loads have to be powered during emergency cases. We also have to face with 5kW of "rejected power" in so far as some of the actuators could be bidirectional (FC in closure operation for instance)
- A 28V LVDC (Low Voltage Direct Current) bus supplying electronic calculators equivalent to an estimated constant load of 4kW.

While the RAT is assumed to be connected to the HVDC bus, the storage device is lead to be connected between those two buses at a "Medium Voltage". As shown on Figure 1, a particular solution could also be considered with the accumulators directly plugged on the LVDC bus. Thus it becomes necessary to study and size the power converters units that have to be implemented depending on the chosen "Middle Voltage". The work presented in this paper aims at estimating the best connection voltage of the accumulators in terms of mass and efficiency for the embedded power electronics. It also takes into account the mass of the considered storage device advised by the manufacturer. The paper mainly refers to the models used to design the components that are connected in the power converter units. Some first results are presented to establish the optimal connection voltage.

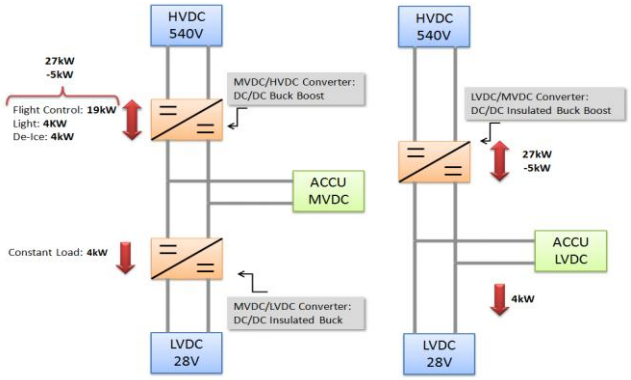

Fig. 1. Scheme of the considered network

2. TOPOLOGİES

2.1. 'NON INSULATED' BUCK BOOST TOPOLOGY

The first topology used to ensure the MVDC/HVDC conversion is equivalent to a

classical bidirectional Boost converter with IGBT/Diode modules (Fig.2). It is here sized for 27kW in boost Mode and 9kW in Buck Mode. We also take into account the possibility to interleave several branches or switches in parallel. It allows us to estimate weight and losses on a wide range of structures and sizing that fulfil the requirements for different connection voltages on the MVDC bus.

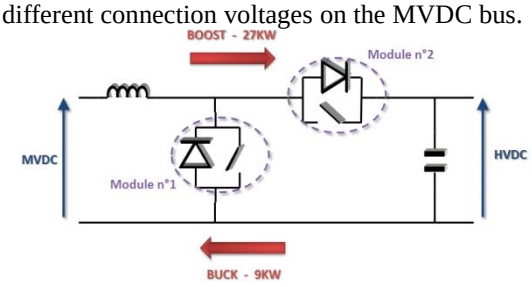

Fig. 2. Non insulated topology

Electrical values such as current ripple, rms or average currents in switches, inductance, capacitance etc... are calculated using basic equations referring to classical Boost converter [4].

2.2 'Insulated' Buck Boost Topology

The second topology is a dual H-Bridge insulated bidirectional DC/DC converter with MOS/Diode modules on the low voltage bridge and IGBT/Diode on the medium voltage side (Fig.3). It is considered as a solution for the MVDC/LVDC conversion as well as the LVDC/HVDC conversion in the case of accumulators connected on the LVDC bus.

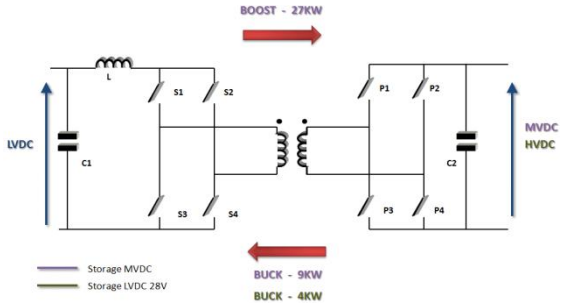

Fig. 3. Insulated topology

The time operation of the voltage transformation from input to output stage can be summarized in Figure 4 with a low voltage of 28V and a medium voltage of 270V[5].

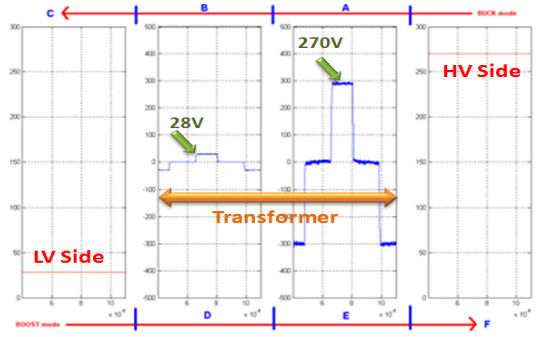

Fig. 4. Voltage Waveforms

- **<u>Boost Mode</u>**

In Boost Mode, only the switches on the low voltage side are controlled while the other bridge could be assimilated to a diode rectifier.

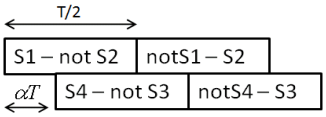

In that case, *Ve-Ie* are respectively the LVDC voltage and current, and *Vs-Is* the HVDC ones. We also use *P* as the sizing power, *m* the turn ratio of the transformer, I_{MAG} being the estimated magnetizing current, *f* the switching frequency. Assuming continuous conduction mode, we calculate:

- Transfer function:

$$\frac{Vs}{Ve} = \frac{m}{(1-2\alpha)}$$

- Inductance:

$L = \dfrac{\alpha Ve}{\Delta IL \times f_{dec}}$ calculated for a duty cycle equal to 1.

$$IL_{\max} = Ie + \frac{\Delta IL}{2} = \frac{P}{Ve} + \frac{\Delta IL}{2} \text{ and } IL_{RMS} = \sqrt{Ie^2 + \frac{\Delta IL^2}{12}}$$

- Capacitor:

$$C = \frac{(1-2\alpha)(\Delta IL + \Delta I_{MAG})}{\Delta Vs \times m \times f_{dec}}$$

$$Ic_{RMS} = \sqrt{(1-2\alpha)Ich^2 + 2\alpha Ic_{\max}{}^2 - \frac{2\alpha}{m} Ic_{\max} \Delta IL + \frac{2\alpha}{3m^2} \Delta IL^2}$$

- Switches (with I_{MAG} equal to zero):

$$Is_{moy} = \frac{IL_{moy}}{2} = \frac{Ie}{2} \quad \text{and} \quad Is_{RMS} = \frac{IL_{RMS}}{\sqrt{2}}$$

$$Ip_{moy} = \frac{\left(\frac{1}{2} - \alpha\right) Ie}{m} \quad \text{and} \quad Ip_{RMS} = \frac{1}{m}\sqrt{Ie^2\left(\frac{1}{2} - \alpha\right) + \Delta IL^2\left(\frac{1-2\alpha}{24}\right)}$$

- Transformer:

$$I1_{RMS} = \sqrt{(1-2\alpha)Ie^2 + \Delta IL^2\left(\frac{7-14\alpha}{6}\right) + 2\alpha I_{MAG}{}^2}$$

$$I2_{RMS} = \frac{\sqrt{2}}{m}\sqrt{Ie^2\left(\frac{1}{2} - \alpha\right) + \Delta IL^2\left(\frac{1-2\alpha}{24}\right) + \Delta I_{MAG}{}^2\left(\frac{1-2\alpha}{24}\right) + \Delta I_{MAG}\Delta IL\left(\frac{5-10\alpha}{24}\right)}$$

- **Buck Mode**

In that mode, both low and high voltage switches have to be controlled. The following sequences have been selected:

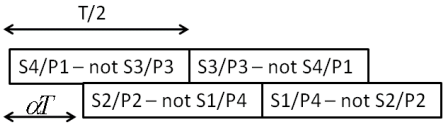

Electrical values for the embedded components are calculated just like previously in a continuous conduction mode. In that case the input voltage *Ve* is the HVDC while *Vs* is the MVDC or LVDC if the accumulators are directly connected at 28V.

- Transfer function:

$$\frac{Vs}{Ve} = \frac{2\alpha}{m}$$

- Inductance:

$$L = \frac{(0.5-\alpha)Ve}{\Delta IL \times f_{dec}}$$

$$IL_{max} = Is + \frac{\Delta IL}{2} = \frac{P}{Vs} + \frac{\Delta IL}{2} \text{ and } IL_{RMS} = \sqrt{Is^2 + \frac{\Delta IL^2}{12}}$$

- Capacitor:

$$C = \frac{\Delta IL}{8\Delta Vsf} \text{ and } Ic_{RMS} = \sqrt{\frac{\Delta IL^2}{12}}$$

- Switches (I_{MAG} =0):

$$Is_{moy} = \frac{IL_{moy}}{2} = \frac{Is}{2} \text{ and } Is_{RMS} = \frac{IL_{RMS}}{\sqrt{2}}$$

$$Ip_{moy} = \frac{\alpha Is}{m} \text{ and } Ip_{RMS} = \frac{1}{m}\sqrt{\alpha Is + \alpha\frac{\Delta IL^2}{12}}$$

- Transformer:

$$I1_{RMS} = \frac{\sqrt{2}}{m}\sqrt{\alpha Ich^2 + \alpha\frac{\Delta IL^2}{12} + \alpha\frac{\Delta I_{MAG}{}^2}{12} + \alpha\frac{\Delta I_{MAG}\Delta IL}{6} + \frac{\Delta I_{MAG}{}^2}{8}(1-2\alpha)}$$

$$I2_{RMS} = \sqrt{2\alpha Ich^2 + \frac{7\Delta IL^2}{6}}$$

For both Boost and Buck mode we have to take into consideration the number of interleaved branches as well as the number of switches connected in parallel. The duty cycle is calculated with the input/output voltage. If it is below 0.5 the previous formulas remains applicable. On the contrary, if the calculated duty cycle α over 0.5, the formula are used and we replace $\alpha' = 0.5 - \alpha$

2.3 DESIGN STRATEGY

The mass and efficiency of the embedded power converter will depend on the voltage connection of the accumulators. In order to appreciate the best solution, power electronics corresponding to various solutions have to be sized. Once the MVDC voltage is entered and the numbers of interleaved branches and switches are defined, we calculate electrical characteristics using the above formulas. The design strategy is presented on Figure 5.

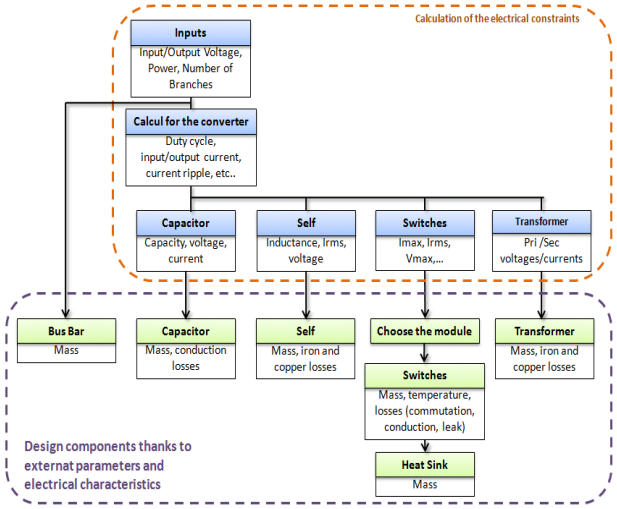

Fig 5. Design Strategy

The mass and efficiency of the whole converter are estimated from the design of the components [6]:

$$W_{Convert} = 1{,}35 \times \sum W_{Components}$$

$$\eta_{CVS} = \frac{P - \sum losses}{P}$$

3. MODELS USED TO DESIGN THE DEVICES

3.1 CAPACITORS

Weight (*Wc*) and internal resistance (*Rc*) of capacitors are calculated with the maximum voltage and the desired capacity using formulas established from datasheets:

$$Wc = 4.36.10e^{-2} \times V + 214.17 \times C^{0.124}$$

$$Rc = 4.29.10e^{-4} \times V + 0.66 \times C^{0.073}$$

3.2 BUS BAR

The weight of the bus bar is given by the following formula [6]:

$$W_{bb} = \frac{1.33}{6} \times nb_{// Branches} \times nb_{// Switches}$$

3.3 SWITCHES

Switching, conduction and leakage losses for both IGBT/Diode modules and MOS/Diode modules are calculated like in [6] taking into account the ratio between test conditions and electrical values calculated in our application. For instance, the following formula is used to estimate the IGBT switching losses:

$$PSwitch_{IGBT} = (Eon(I_{IGBT}) + Eoff(I_{IGBT})) \times f \times \frac{V_{IGBT}}{V_{Test}}$$

In the same time, we get an idea of the mass of the embedded silicon and the temperature at the base of the components is determined with the calculated losses and the following model (Fig.6).

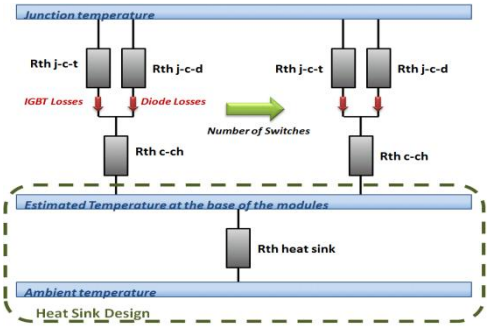

Fig 6. Thermal Model for IGBT/Diode Modules

3.4 HEAT SİNK

We consider a forced convection cooling system and a dissipator with winglets (Fig.7) in order to ensure an operating temperature below the maximum junction temperature.

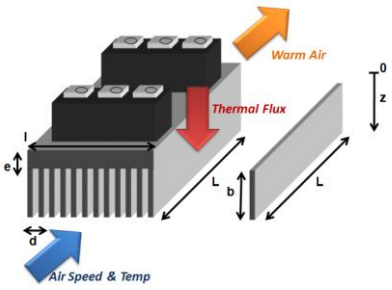

Fig. 7. Considered Heat Sink

We consider heat transfer problems and especially the Newton's law giving the thermal energy exchanged between the ambient pulsed air and the heat sink with *h* the heat transfer coefficient (W/m²) and *S* the heat exchange area:

$$\Phi = hS(T_{HeatSink}(z) - T_{Air})$$

Where $T_{HeatSink}(z) = \frac{T_{Air} - T_{Module}}{b} z + T_{Module}$

The thermal energy that could be dissipated by the designed heat sink in operating conditions will be mainly estimated through the value of the heat transfer coefficient *h*. That value is taken from a dimensionless number called the Nusselt number (*Nu*). It is extrapolated using the Colburn correlation for a turbulent flow, with the Reynolds (*Re*) and Prandtl (*Pr*) numbers that define the characteristics of the flow at a given temperature and speed [7]. With λ the conductivity of the fluid:

$$\overline{Nu} = 0.023\,\mathrm{Re}^{0.8}\,\mathrm{Pr}^{0.33} \text{ and } Nu = \frac{h2d}{\lambda}$$

Once the Nusselt number is known, we calculate the total heat energy dissipated with the following formula where nb_{wing} is the number of winglets:

$$\Phi = hL(b+d)(T_{Module} - T_{Amb})(nb_{Wing} - 1)$$

The design of the component is optimized in terms of mass checking that all losses are dissipated and that the flow remains turbulent (*Re* over 10000).

3.5 INDUCTORS

The chosen cores for inductors are U cores in ferrite (3C90) with flat conductors. The air gap *e* is distributed in the structure as shown on Figure 8. With the geometry of the circuit, we calculate the magnetic reluctance with a permeability depending on a magnetic field define as B_{calc}. Hence, we access to the true magnetic field with the operating conditions. Once the alternative component of the magnetic field is known, iron losses are estimated using the Steinmetz formula where T_{calc} is the supposed temperature of the component [8] [9]:

$$dP_{fer} = Cm \times f^{x} \times \left(\frac{B_{AC}}{2}\right)^{y} \times (ct0 - ct1T_{calc} + ct2T_{calc}^{2})$$

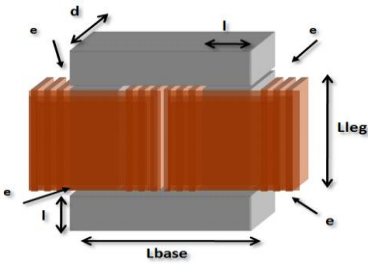

Fig. 8. Considered Inductor

The direct resistance of the conductors is calculated with a resistivity ρ depending on the operating temperature T_{calc}, *Nt* being the number of turns, with the thickness of both conductors (*ec*) and insulation (*dc*)

$$R_{DC} = \frac{\rho \times \left(Nt(d + l + 2dc) + \frac{(Nt-1)Nt}{2}(ec + dc)\right)}{L_{leg} \times ec}$$

The alternative resistance is with the Dowell's model given for transformer winding with the skin depth δ [10]:

$$F_R = \frac{R_{AC}}{R_{DC}} = X\frac{\sinh 2X + \sin 2X}{\cosh 2X - \cos 2X} + 2X\frac{m^2-1}{3}\frac{\sinh X - \sin X}{\cosh X + \cos X}$$

Skin Effect — Proximity Effect

where $X = \frac{ec}{\delta}$ and m is the number of layers in the winding .

Then the heating of the component is calculated with the Newton's law where h=5W/m²K that corresponds to average natural convection according to [7]. The heat transfer area S is assumed to be the overall surface of the sized component.

$$T_{Induc} = T_{Amb} + \frac{1}{hS} \times Losses$$

The design is optimized in term of mass and we pay attention to the difference between T_{calc} and T_{Induc} and between B_{calc} and B_{Induc} that have to be below 5%. In addition, many constraints have to be respected such as overheating, saturation of the ferromagnetic material, current density, area product.

3.6 TRANSFORMERS

The sizing strategy for transformers is very similar to the previous one presented for inductors (Fig.9).

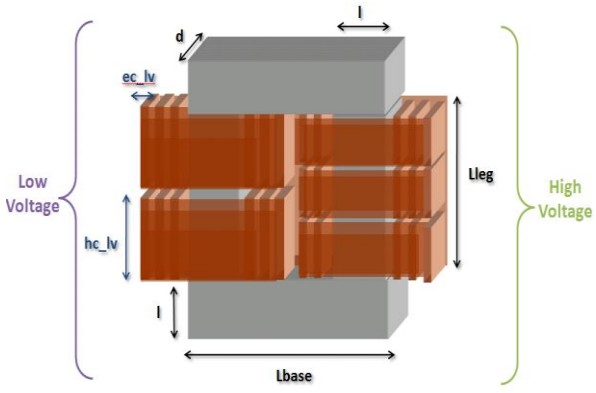

Fig. 9. Considered Transformer

One main difference is noticed for the copper losses. For each winding, we calculate the number of layers depending on the number of turns Nt and the geometry.

$$Nb_{layers} = ENT\left(\frac{Nt}{ENT\left(\frac{Lleg}{hc}+1\right)}+1\right)$$

$$R_{DC} = \frac{\rho \times \left(Nt(d+l+2dc) + \frac{(Nb_{layers}-1)Nb_{layers}}{2}(ec+dc) \times ENT\left(\frac{Lleg}{hc}+1\right)\right)}{hc \times ec}$$

The same constraints have to be respected in the case of the transformers. In addition, we have to control the turn ratio as well as the value of the magnetizing current below 5% of the current flowing in windings on the low voltage side.

4. RESULTS OF SIZING

All the previous models have been implemented in the same tool in order to estimate the weight of power electronics corresponding to different connection voltages of the storage device. The design has been processed with a switching frequency at 20kHz, an ambient temperature at 50°C, a maximal junction temperature of switches at 125°C, a maximal temperature of magnetic cores at 150°C and a air speed in the heat sink at 10m/s. Some hypotheses also remain the same whatever the considered solution. The maximum voltage ripple is fixed at 1% while the current ripple should not exceed 10%.

4.1 LVDC ACCUMULATOR

For this network configuration (right part of Fig.1), a LVDC (28V)/HVDC (540V) isolated Buck Boost power converter (BBCU) is used. The design strategy has allowed obtaining a mass of 34 kg and 80% for efficiency. The mass of the 28V battery is estimated at 48kg.

4.2 MVDC ACCUMULATOR

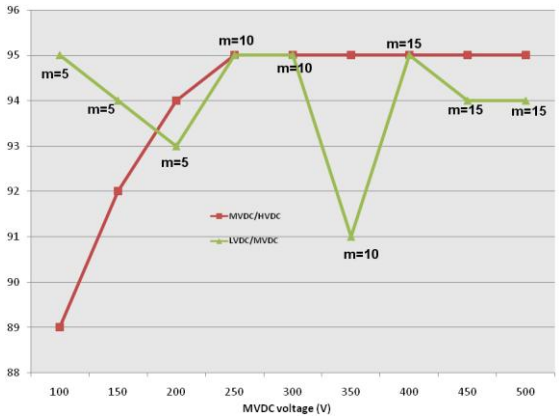

Fig. 10. Efficiency of power converters (%)

Both insulated and non-insulated converters are needed for this strategy of connection (left part of Fig.1). The Figure.10 refers to the evolution of efficiencies for both power converters according to the MVDC voltage. Increasing the MVDC voltage is better for the efficiency of the non-insulated topology that ensures the MVDC/HVDC conversion (reduced power losses in power switches). For the insulated buck converter, the

turns ratio of the transformer *m* has a major impact and we notice that losses in the switches and in the transformer are the most significant. The mass of the insulated power converter increases with the MVDC voltage whereas it is the opposite for the buck/boost converter (Fig.11). For both insulated and non-insulated topologies most of the mass is caused by the magnetic components. Thus it could be interesting to study the sensitivity of the model versus parameters such as heat transfer coefficient or saturation of the magnetic material but it is not discussed in the present paper.

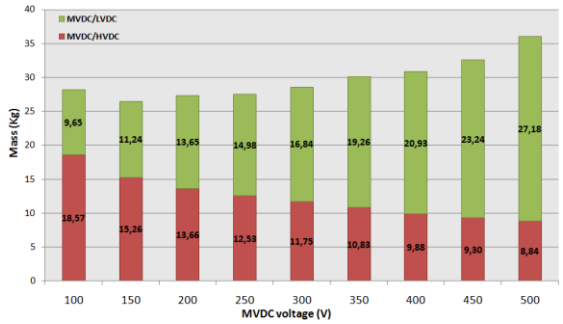

Fig. 11. mass of the power converters

4.3 MASS OF THE SYSTEM.

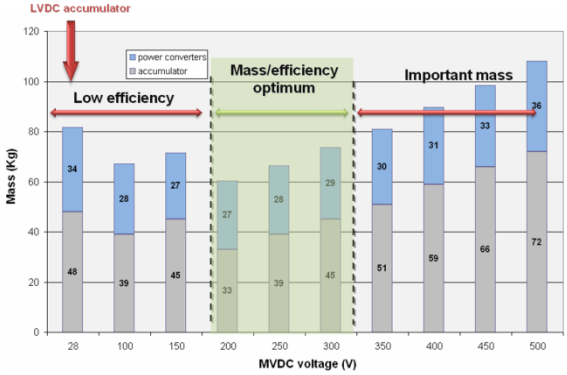

Fig. 12. mass of the overall system

The Figure 12 presents the mass of the system versus the connection voltage. At high connection voltages the mass of the accumulator increases with the voltage because there are more cells in series whereas at low levels we have to connect several branches in parallel to ensure the mission in term of energy which also led to a mass increase. Finally the optimum for the connection voltage appears to be between 200V and 300V.

5. CONCLUSION

In this paper, we have developed basic models for the components of power converter units. Using simple hypotheses, we have processed a pre-sizing in terms of mass and efficiency that has proved to be valuable to determine the best connection voltage of the storage device. The design strategy is optimized for the heat sink and magnetic components. In a further development, we could process a multiobjective optimization to find for each voltage the approriate number of interleaved branches or switches, and the best turn ratio.

6. ACKOWLEGMENT

This study has been involved in the framework of the ISS (Innovative Solution for Systems) national project for which the authors thank the DGAC (Direction Générale de l'Aviation Civile) and Airbus operation SAS for support and funding. Authors also like to thank SAFT for scientific cooperation.

7. REFERENCES

[1] JA Rosero, JA Ortega, E Aldabas, L Romeral, Moving towards a more electric aircraft, IEEE Aerospace and Electronic System Magazine, Vol 22, Issue 3, pp 3-9, March 2007.

[2] O Langlois, Conception d'un réseau de secours électrique pour l'aéronautique, PhD, Institut National Polytechnique, Toulouse, June 2006,http://ethesis.inp-Toulouse.fr/archive/ 00000243/.

[3] K Rafal, B Morin, X Roboam, E Bru, C Turpin, H Piquet, Experimental Electrical Network for Aircraft Application, IEEE VPPC'10 conference, Lille, France, September 2010.

[4] RW Erickson, D Maksimov, Fundamental of Power Electronics, Springer, 2001.

[5] L Rubino, B Guida, P Marino, A Cavallo, On the selection of optimal turn ratio for transformers in isolated DC/DC boost full bridge converter, SPEEDAM 2010 International Symposium on, Pisa, Italy, pp. 39-43, June 2010.

[6] M Garcia Arregui, Theoretical study of a power generation unit based on the hybridization of a fuell cell stack and ultracapacitors, PhD, Institut National Polytechnique, Toulouse, December 2007, http://ethesis.inp-oulouse.fr/archive/00000521/.

[7] A Bejan, AD Krauss, Heat Transfer Handbook, Willey-IEEE, 2003

[8] M Sippola, RE Sepponen, Accurate prediction of high-frequency power-transformer losses and temperature rise, IEEE Transcations on Power Electronics, Vol 17, no5, pp. 835-847, September 2002.

[9] Design of Planar Power Transformers, Application Note, Ferroxcube, 1997.

[10] PL Dowell, Effects of eddy currents in transformer windings, Proceedings IEE, vol.133, n°8, pp. 1387-1394, August 1966.